Optical Materials 129 (2022) 112518

Contents lists available at ScienceDirect

Optical Materials

journal homepage: www.elsevier.com/locate/optmat

Research Article

Photoluminescence downshifting studies of thermally stable Dy^{3+} ions doped phosphate glasses for photonic device applications

Kartika Maheshwari [a,b], A.S. Rao [a,*]

[a] Department of Applied Physics, Delhi Technological University, Bawana Road, Delhi, 110042, India
[b] ABES Engineering College, Ghaziabad, Uttar Pradesh (U. P.), 201 009, India

ARTICLE INFO

Keywords:
Glasses
Dysprosium ions
XRD
Photoluminescence
CIE coordinates
Temperature-dependent photoluminescence

ABSTRACT

Trivalent dysprosium (Dy^{3+}) activated barium zinc lithium phosphate (BaZnLiP) glasses were prepared by employing melt quench routes. To understand the possible applicability of the prepared glasses in photonic device applications, numerous structural, optical, and radiative characteristics have been explored in detail. The non-crystalline character of BaZnLiP glass has been confirmed with the help of an X-ray diffraction pattern. The titled glasses doped with Dy^{3+} ions show several absorption peaks in the 330–1800 nm range with an indirect optical band gap of 3.41–3.76 eV. The Judd-Ofelt (J-O) theory was employed on the absorption profiles and estimated various radiative parameters for the Dy^{3+} ions activated BaZnLiP glasses. The Dy^{3+} ions activated glasses exhibit intense excitation at 350 nm and three sharp visible emissions at blue ($^4F_{9/2} \rightarrow {}^6H_{15/2}$), yellow ($^4F_{9/2} \rightarrow {}^6H_{13/2}$), and red ($^4F_{9/2} \rightarrow {}^6H_{11/2}$). To ascertain the lasing potentialities of BaZnLiP glasses, the stimulated emission cross-section and branching ratios have been assessed by correlating the emission spectral information with the radiative parameters calculated from the absorption spectral features. The colorimetric properties show the coordinates situated in a bright white region. Temperature-dependent photoluminescence (TD-PL) spectral features recorded revealed the thermal stability of the as-prepared glasses. The explored distinctive features for Dy^{3+} ions activated BaZnLiP glasses suggested the superiority and direct utility of the as-prepared glasses in advanced photonic device applications such as lasers and w-LEDs.

1. Introduction

Recently, enormous research has been focused on the non-crystalline glasses activated with rare-earth (RE) ions owing to their excellent features such as high transparency, low manufacturing cost, easy fabrication technique, highly durable, excellent emission properties, and high thermal stability. RE ions activated glasses have direct utility in numerous areas such as solid-state lasers, optical fibers, sensors, light converters, and other optoelectronic devices [1]. The spectroscopic investigations for instance absorption, PL excitation, PL emission, PL decay, and TD-PL features recorded for the RE ions doped glasses explore the utility of the host glass matrix for the aforementioned various photonic devices applications. The spectral features of the active ions (RE ions) doped into a host matrix can be varied by appropriate choice of host matrix composition or by varying the RE ion concentration in a host. RE ions doped glasses have distinct optical properties in various host glasses like phosphate, borate, silicate, telluride, and chalcogenides from the perspective of their applications in solid-state lasers [2–4]. To enhance the lasing properties, the glass host can be formed by using a good glass former added with intermediates and network modifiers [5,6]. For the best optical and lasing properties, the selection of host glass with various RE ions is a still difficult task [1]. To increase the stimulated emission cross-section and quantum efficiency, host glass with low phonon energy is very much essential. A host glass with relatively less phonon energies can increase radiative properties by suppressing the non-radiatve decay process [7].

In quite recent times w-LEDs replace traditional fluorescent and incandescent lamps. These w-LEDs serve many purposes, including excellent durability, less power consumption, and a longer life span [8]. For the commercial availability of w-LEDs, phosphors activated by the blue LED chip to emit green and red lights alternately are usually employed. The majority of current research, on the other hand, is focused on white emission by UV excitation without the usage of an LED chip. RE doped glasses provide many advantages, including decreased manufacturing costs, a straightforward manufacturing process, and no halo effect [9].

* Corresponding author.
E-mail address: drsrallam@gmail.com (A.S. Rao).

https://doi.org/10.1016/j.optmat.2022.112518
Received 4 February 2022; Received in revised form 15 May 2022; Accepted 19 May 2022
Available online 30 May 2022

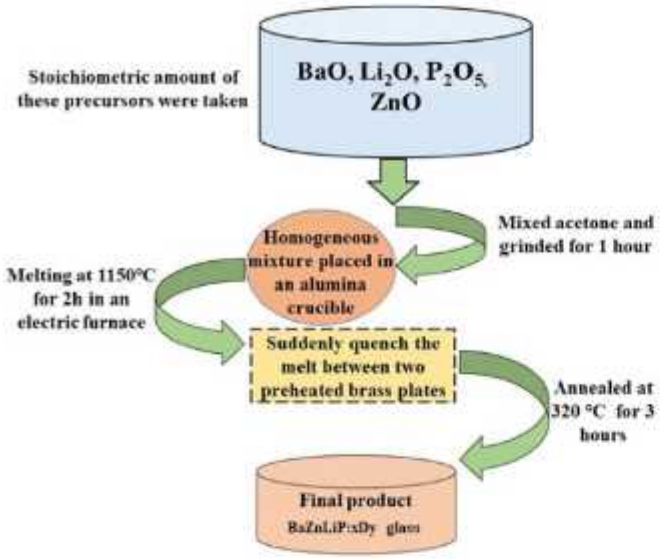

Fig. 1. Schematic diagram of melt quenching technique used to prepare BaZnLiP glasses.

There are various glass formers like fluorides, phosphates, borates, tellurites, silicates, borosilicate, etc. The researchers working in the field of glass science & technology have prepared a variety of glasses using the above-mentioned glass formers along with network formers and studied their spectroscopic properties. Among various glass formers, phosphate is one of the suitable glass formers owing to distinctive properties like clear visibility in the wide-ranging spectrum, softening, less melting temperature, high thermal stability, high RE ion solubility, and low dispersion [10]. Phosphate glasses possess various applications in photonic devices but it has some limitations because of their hygroscopic nature and poor chemical stability [11]. To overcome these limitations, network modifiers (BaO, Li_2O) and intermediate (ZnO) have been added to the host glass, which can increase chemical stability and reduce thermal expansions. Moreover, ZnO helps to overcome hygroscopic nature and increases the solubility of RE ions. All the above-discussed characteristic features possessed by the chemical species P_2O_5, Li_2O, BaO, and ZnO prompted us to prepare a glassy system namely barium zinc lithium phosphate (BaZnLiP) glass. Phosphate-based glasses doped with RE ions are effective in improving the luminescent characteristics of a material to have potential applications in the field of optoelectronics [12–15].

Dy^{3+} is one of the very attractive RE ions for fabricating visible solid-state devices as its emission takes place in the visible region due to f-f transitions. In general, Dy^{3+} doped materials have two major peaks in blue and yellow regions, and if their intensity ratio is appropriate, then Dy^{3+} ions doped materials show a white light. The Y/B ratio can be enhanced by changing Dy^{3+} ions concentration and excitation wavelength, which further gives magnificent emission from glassy materials in the visible region [16–20]. Recently, S. Tian et al. investigated silicate-clad Dy^{3+} doped multi-component phosphate glass core glass fiber for yellow laser applications. The sample with 1 mol.% Dy_2O_3 (2.6 wt%) doping concentration exhibits the most intensive yellow emission and its internal quantum efficiency was determined to be 39.27% [21]. P. Babu et al. prepared Dy^{3+} ions doped zinc oxyfluorotelluride glasses. The CIE coordinates of as-prepared T20ZofNDy1.0 glass are very nearer to the white light region, showing their applications in w-LEDs [22]. R.J. Amjad and his co-workers synthesized Dy^{3+} doped PbO–ZnO–B_2O_3–P_2O_5 glasses for white light-emitting materials and solid-state laser applications [23].

In the present research work, BaZnLiP glasses doped with varying concentrations of Dy^{3+} ions were prepared by using the melt quench route. Various spectroscopic characterizations were performed on Dy^{3+} ions doped BaZnLiP glasses to explore their structural, optical absorption, PL properties, and thermal stability. The J-O theory has been applied to the measured absorption bands (called oscillator strengths) useful in assessing various radiative properties for the prominent fluorescent levels of Dy^{3+} ions in the titled glasses. Further, the absorption and emission properties are correlated to understand the lasing potentialities of the titled glasses. TD-PL spectral features are recorded to understand the thermal stability of the titled glasses. Colorometric studies were also conducted on the titled glasses to understand the usage of the titled glasses in lighting industry as epoxy-free w-LEDs.

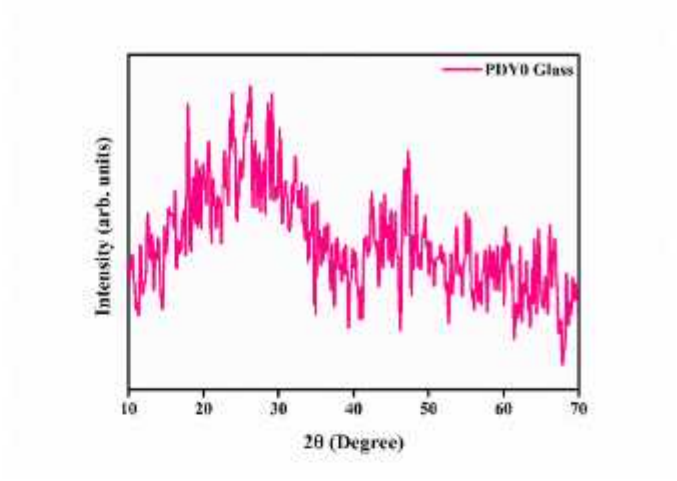

Fig. 2. XRD pattern of an undoped BaZnLiP glass.

2. Experimental procedure and characterization

BaZnLiP glasses doped by varying concentration of Dy^{3+} ions in accordance with the molar composition $60P_2O_5$- (15-x)BaO -15ZnO –$10Li_2O$-xDy_2O_3 (x = 0, 0.1, 0.5, 1.0, 1.5 and 2.0 mol% named as PDY0, PDY1, PDY2, PDY3, PDY4 and PDY5 glasses, respectively) were prepared via melt quench approach. The process used to synthesize these phosphate glasses has been depicted in Fig. 1. Further, all the glasses were characterized through various techniques to check their suitability for photonic devices. An X-ray Bruker D8 advance diffractometer with Cu-Kα radiation (=1.5406 Å) having nickel filtered in 2θ angle region $10^{o} \leq \theta \leq 70^{o}$ was used for measuring the X-ray diffraction (XRD) pattern for an undoped BaZnLiP glass. Density and refractive indices of the Dy^{3+} ions doped BaZnLiP glasses were measured by employing the Archimedes principle and Brewster's angle method respectively. Absorption spectra for doped BaZnLiP glasses were recorded in the 330 nm–1850 nm wavelength range by using a JASCO-made V-770 UV–VIS spectrometer. The PL excitation and emission properties of Dy^{3+} activated BaZnLiP glasses characterize through JASCO FP-8300 Spectro fluorometer attached to the Xenon arc lamp. PL decay curve recorded by using Edinburgh FLSP 980 Spectro fluorophotometer with an excitation source as Xenon flash lamp. TD-PL spectra were recorded with a spectrometer (Ocean Optics) connected with a Xenon excitation source and a sample holder attached with heating assembly.

3. Results & discussion

3.1. Structural analysis

The XRD pattern recorded for an undoped BaZnLiP glass in angular range (10–70°) has been depicted in Fig. 2. It shows a wideband rather than distinguish sharp peaks, which indicates the non-crystalline character of BaZnLiP glass.

Table 1
Various physical properties of Dy^{3+} ions in BaZnLiP glasses.

S. No	Physical Property	PDY1	PDY2	PDY3	PDY4	PDY5
1	Refractive index (n_d)	1.60	1.60	1.59	1.599	1.59
2	Density (gm/cm^3)	2.88	2.89	2.90	2.91	2.92
3	Average molecular weight	123	124	125	126	127
4	Dy^{3+} ion concentration, N (10^{22} ions/cm^3)	0.14	0.70	1.39	2.08	2.77
5	Molar Volume (cc/mol)	42.70	42.90	43.10	43.29	43.49
6	Mean atomic volume (g/cm^3/atom)	8.36	8.38	8.39	8.41	8.42
7	Dielectric constant (ε)	2.56	2.56	2.55	2.55	2.55
8	Optical dielectric constant ($\varepsilon - 1$)	1.56	1.56	1.55	1.55	1.55
9	Reflection losses (R %)	5.32	5.32	5.32	5.32	5.32
10	Molar refraction (R_m) (cm^{-3})	14.59	14.67	14.73	14.80	14.86
11	Polaron radius (r_p) (Å)	3.59	2.10	1.67	1.46	1.33
12	Inter-atomic distance (r_i) (Å)	8.92	5.22	4.15	3.63	3.30
13	Molecular electronic polarizability (10^{-22} cm^3)	5.79	1.16	0.58	0.39	0.29
14	Field Strength F (X10^{15}cm^{-2})	2.32	6.77	10.7	14.0	16.9

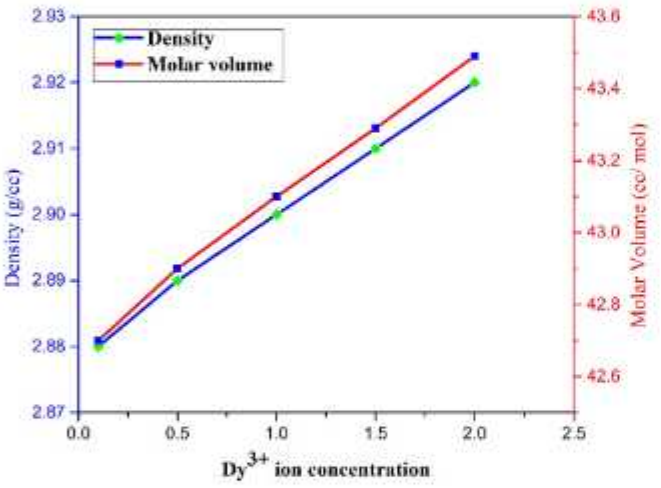

Fig. 3(a). Density and molar volume variation with Dy^{3+} ions concentration in BaZnLiP glasses.

3.2. Physical properties

Several physical and optical characteristics for BaZnLiP glasses were assessed using the relevant mathematical expressions given in the literature and are given in Table 1 [5]. It is noted for BaZnLiP glasses, as the Dy^{3+} ions concentration is increasing from PDY1 (0.1 mol%) to PDY5 (2.0 mol%), substantial quantities such as density, mean atomic weight, molar volume, molar reflection, and field strength are increasing, while others such as refractive index, optical dielectric constant, reflection loss (R%), polaron radius, mutually distance between atoms (r_i), and electronic polarizability are reducing. Densities for BaZnLiP glasses increase because the molecular weight of host compounds i.e., P_2O_5 (141.94 g/mol), ZnO (81.37 g/mol), BaO (153.33 g/mol), and Li_2O (29.88 g/mol) is lower than that of Dy_2O_3 (372.9 g/mol) which reveals the degree of structural closeness in BaZnLiP glasses [24,25]. The average molecular weight of BaZnLiP glasses is also escalating due to the addition of Dy_2O_3 in the host glass. The variation of density and molar volume along with varying Dy^{3+} ion concentration in BaZnLiP glasses is represented in Fig. 3(a). From Fig. 3(a), it is conspicuous that density and molar volume is surging as the concentration

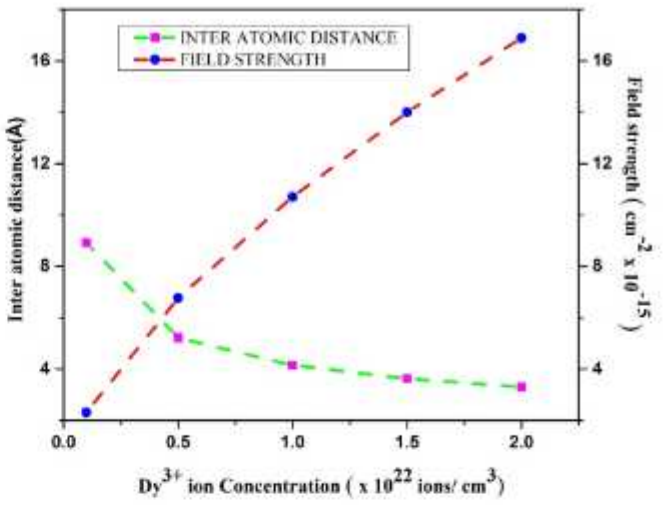

Fig. 3(b). Variation of inter atomic distance and field strength with Dy^{3+} ions concentration in BaZnLiP glasses.

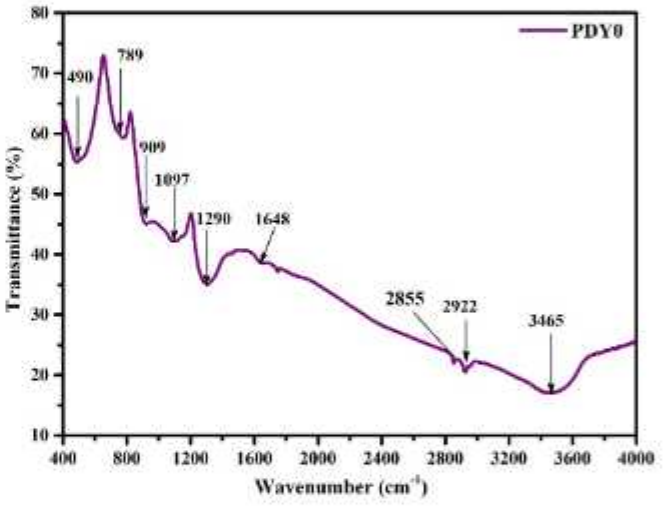

Fig. 4. FT-IR spectrum of an undoped BaZnLiP glass.

of Dy^{3+} ions increases. With an increase in Dy^{3+} ions concentration, the number of dysprosium ions per unit volume also increases in host glass which in turn leads to an increase in molar volume and other physical properties. Furthermore, in the present work, alkaline earth oxide(Li_2O) is added to enhance the stability of the glass network by bridging oxygen atoms with Dy^{3+} ions. The interatomic distance decreases as the concentration of Dy^{3+} ions increases for the prepared glasses. The decrease in interatomic distance results in the surge of field strength. The interatomic distance and field strength shows an inverse relationship with an increase in the concentration of Dy^{3+} ions in BaZnLiP glass as shown in Fig. 3(b). Comparatively, low values of field strength for BaZnLiP glasses represent the high solubility of Dy^{3+} ions in the host glass. Molecular electronic polarizability is another important physical property that relates to optical, chemical, and dielectric properties like UV absorption, ionic reflection, and chemical stability. BaZnLiP glasses with relatively low values of molecular electronic polarizability help in increasing its stability.

3.3. Vibrational spectroscopy

Fourier Transform Infrared spectroscopy (FT-IR) spectrum recorded for an undoped BaZnLiP glass (PDY0) within the 400–4000 cm^{-1} range

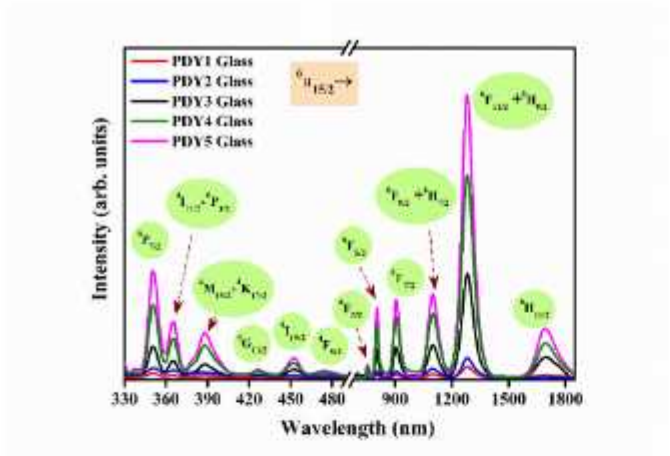

Fig. 5. Absorption spectra of Dy^{3+} ions doped BaZnLiP glasses in UV–vis–NIR region.

has been depicted in Fig. 4. The FT-IR spectrum displayed in Fig. 4 shows several peaks situated at 490, 789, 909, 1097,1290,1648, 2855, 2922, and 3465 cm^{-1}. The band at 490 cm^{-1} may be assigned due to bending of PO_2 vibrations and also tetrahedral bond stretching of Zn–O [26]. Other bands located at 789 cm^{-1} and 909 cm^{-1} may be attributed due to symmetric stretching (υ_s) and asymmetric stretching, (υ_{as}) of PO_2 connection of Q_1 tetrahedral and Q_2 tetrahedral respectively with non-bridging oxygen atoms [11,27]. The band at 1097 cm^{-1} may be due to asymmetric stretching of Q_2 tetrahedral vibrating in PO mode, υ_{as} ($P–O^-$) and maybe resembled as a linkage of the P–O–Zn stretching band [28]. The band at 1290 cm^{-1} is ascribed due to stretching vibrations of P–O bonds in PO_4 units. The band at 1648 cm^{-1} is ascribed due to O–H bending vibrations integrated because of air present in the making of KBr pellets for FT-IR characterization [29]. The band at 2855 cm^{-1} represents the presence of carbon contaminants [30]. The band observed at 2922 and 3465 cm^{-1} are on account of asymmetric and symmetric vibrations of the H_2O molecules respectively [31].

3.4. Absorption spectral analysis

Absorption spectra of Dy^{3+} ions doped BaZnLiP glasses recorded from 330 to 1650 nm wavelength range in UV–vis–NIR region is shown in Fig. 5. The spectra depicted in Fig. 5 show a series of dysprosium absorption peaks observed in UV, Visible, and NIR regions arising from its ground ($^6H_{15/2}$) to numerous higher energy states such as $^6P_{7/2}$, $^4I_{11/2} + {}^6P_{3/2}$, $^4M_{19/2} + {}^4K_{17/2}$, $^4G_{11/2}$, $^4I_{13/2}$, $^4F_{9/2}$,$^6F_{3/2}$, $^6F_{5/2}$, $^6F_{7/2}$, $^6F_{9/2} + {}^6H_{7/2}$, $^6F_{11/2} + {}^6H_{9/2}$ and $^6H_{11/2}$ at wavelengths of 351, 364, 386, 425, 452, 487, 753, 803, 900, 1095, 1278 and 1685 nm, respectively [24]. From Fig. 5, it is conspicuous that, the absorption bands observed in the NIR region (spin allowed) are relatively stronger than the ones observed in the visible region (forbidden). Among various absorption transitions observed in the NIR region, the one pertaining to $^6H_{15/2}$ to $^6F_{11/2} + {}^6H_{9/2}$ detected at 1278 nm follows spin allowed rule $\Delta|S\Delta| ,0 = |L\ 2 \leq|$ and $\Delta|J\ 2 \leq|$ and is highly intense than the other transitions (seeFig. 5).

The indirect optical band gap for Dy^{3+} ions activated BaZnLiP glasses were assessed as per recorded absorption spectra with the help of relation given by Davis and Mott as follows [11]:

$$\alpha h\upsilon = B\left(h\upsilon - E_{opt}\right)^n \quad (1)$$

In the above relation, α denotes the absorption coefficient $h\upsilon$ which represents the incident photon energy, and B signifies the band tailing parameter, E_{opt} which indicates the energy bandgap. The value of the parameter n describes the type of transition having values where $n = ½$ and $n = 2$ for direct and indirect allowed transitions, respectively. The E_{opt} values were acquired for indirect and direct optical transition using Tauc's plot by extrapolating the linear portion of the plot $(\alpha h\upsilon)^n$ versus $(h\upsilon)$ with $n = 1/2$ and $n = 2$ [as presented in Fig. 6(a) and (b)] respectively. The estimated indirect E_{opt} Values were found to be 3.64,

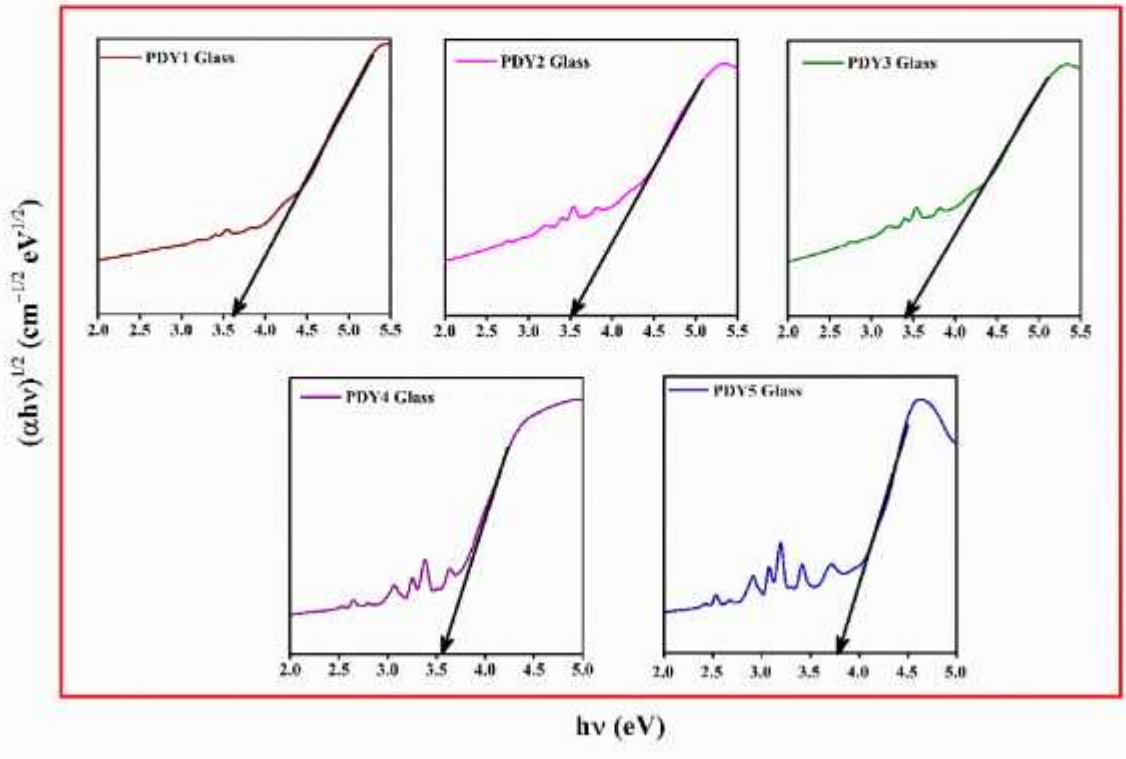

Fig. 6(a). Indirect bandgap plot for Dy3+ ions doped BaZnLiP glasses.

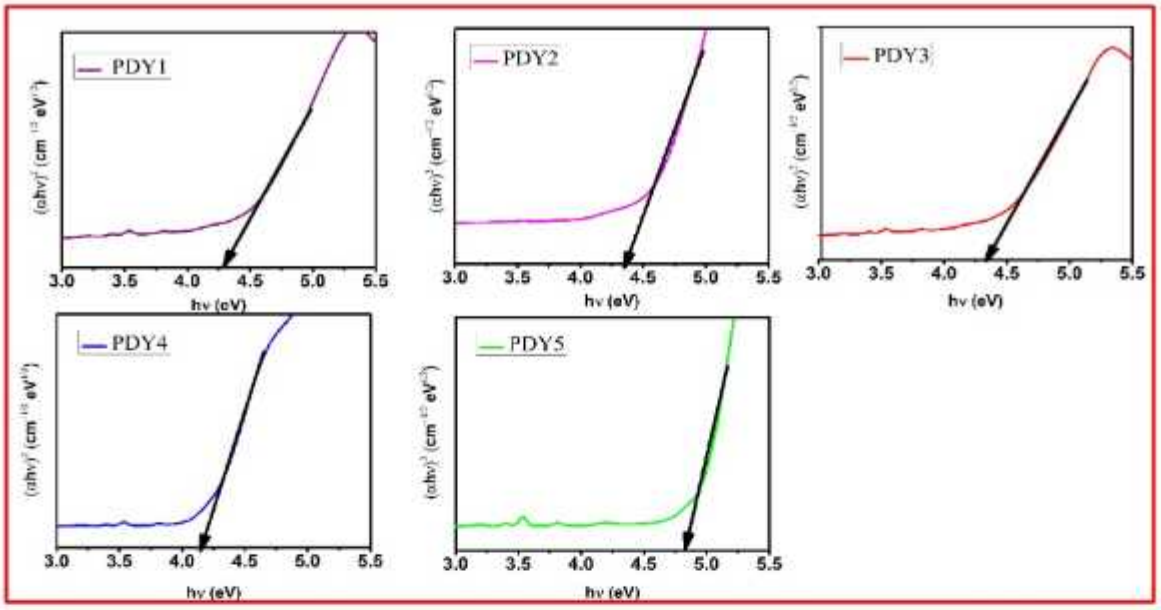

Fig. 6(b). Direct bandgap plot for Dy3+ ions doped BaZnLiP glasses.

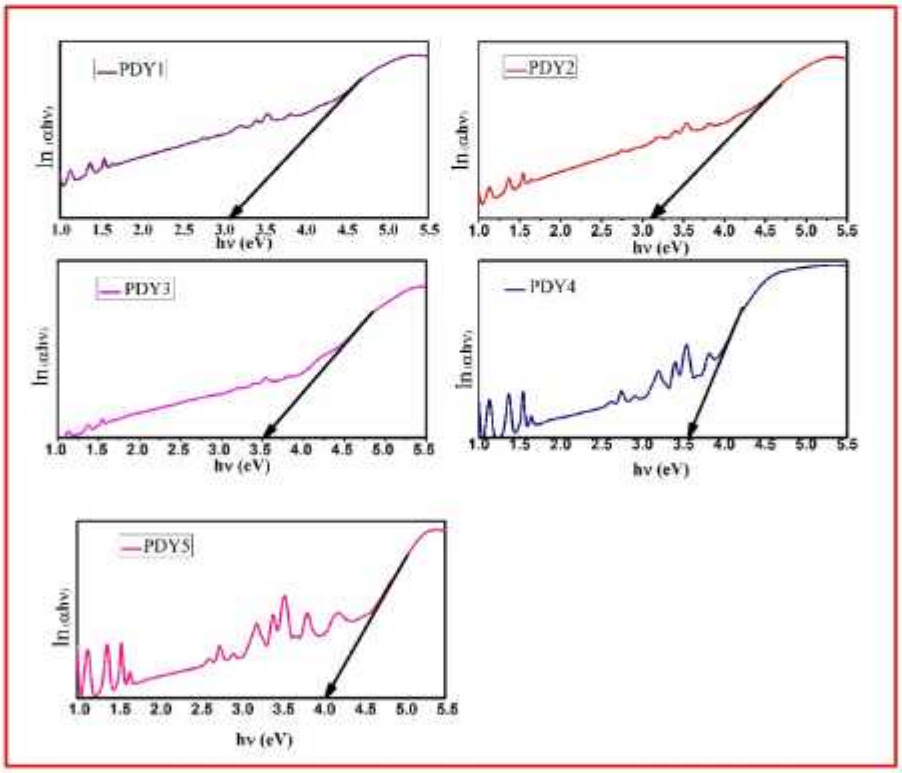

Fig. 6(c). Urbach energy plot for Dy^{3+} ions doped BaZnLiP glasses.

3.53, 3.41, 3.56, and 3.76 eV for PDY1, PDY2, PDY3, PDY4, and PDY5 glasses, respectively. Similarly, the values for direct E_{opt} were 4.28, and 4.33. 4.35,4.16 and 4.83 eV for respective glasses.

Furthermore, in most of the glassy materials, the fundamental absorption edges are identified by the degree of the exponential tail. These absorption edges may arise due to inter-band transitions including tails of the localized states and follow by the Urbach rule [32].

The Urbach rule is explained by the following formula:

$$\alpha(\vartheta) = C exp\left(\frac{h\vartheta}{\Delta E}\right) \quad (2)$$

Where C is constant, ΔE is the Urbach energy represents the width of band tails of localized states. The Urbach energies are evaluated by plotting a graph between ln ($\alpha h\vartheta$) versus $h\vartheta$ and then taking the inverse of the slope of the plotted graph as shown in Fig. 6(c). The values of ΔE are decreasing (0.324, 0.316, 0.283, 0.280, and 0.239 eV) with an

Table 2
Experimental (f_{exp}) (x10^{-6}), calculated (f_{cal}) (x10^{-6}) oscillator strengths, r.m.s deviation (δ_{rms}), nephelauxetic ratio ($\bar{\beta}$), bonding parameters (δ), and refractive index (n_d) for Dy^{3+} ions in BaZnLiP glasses.

Transitions from $^6H_{5/2}$→	PDY1		PDY2		PDY3		PDY4		PDY5	
	f_{exp}	f_{cal}	f_{exp}	f_{cal}	f_{exp}	f_{cal}	f_{exp}	f_{cal}	f_{exp}	f_{cal}
$^6P_{7/2}$	–	–	0.21	1.737	0.3	1.920	1.17	2.701	0.92	2.396
$^4I_{11/2}$ + $^6P_{3/2}$	–	–	0.17	0.045	0.25	0.078	0.65	0.090	0.24	0.069
$^4M_{19/2}$ + $^4K_{17//2}$	0.67	0.361	0.68	0.269	0.86	0.337	0.95	0.379	0.61	0.325
$^4G_{11/2}$	-	–	–	–	0.04	0.054	0.14	0.073	0.06	0.065
$^4I_{13/2}$	0.46	0.269	0.52	0.218	0.54	0.262	0.62	0.282	0.31	0.247
$^4F_{9/2}$	0.41	0.051	0.42	0.028	0.46	0.041	0.55	0.050	0.2	0.040
$^6F_{3/2}$	–	–	0.1	0.023	0.11	0.036	0.12	0.042	0.09	0.0323
$^6F_{5/2}$	0.43	0.293	0.44	0.113	0.51	0.196	0.74	0.224	0.5	0.1721
$^6F_{7/2}$	0.55	0.669	0.8	0.382	1.08	0.551	1.18	0.681	1.07	0.5555
$^6F_{9/2}$ + $^6H_{7/2}$	0.51	0.466	0.96	0.394	1.05	0.491	1.16	0.650	1.05	0.5563
$^6F_{11/2}$ + $^6H_{9/2}$	4.16	4.162	4.56	4.405	5	4.828	5.41	5.231	4.92	4.7588
$^6H_{11/2}$	–	–	0.11	0.716	0.17	0.843	0.21	0.912	0.16	0.8051
δ_{rms} (x 10^{-6})	± 0.25		± 0.55		± 0.60		± 0.62		± 0.52	
n_d	1.600		1.600		1.599		1.599		1.599	
$\bar{\beta}$	0.996		0.995		0.994		0.994		0.993	
δ	0.38		0.49		0.53		0.59		0.61	

increase in the concentration of the doped RE ion concentration from 0.1 to 2.0 mol%. Relatively lower values of ΔE indicates the minimum defect present in the host glass network.

The nephelauxetic effect, an estimation of the covalent character of transition metal-ligand interaction in BaZnLiP glass matrix will appear as partially filled f shells. Electronic orbitals for the 4f configuration are disfigured because Dy^{3+} ions are present in BaZnLiP glass [33]. To get an idea about the bond linking in metal transition ions (Dy^{3+}) and nearby ligands, nephelauxetic ratio (β) and bonding parameters (δ%) are determined by the formula as written below and are given in Table 2 [4].

$$\beta = \frac{\vartheta_c}{\vartheta_a} \tag{3}$$

where ϑ_c and ϑ_a are the wavenumbers corresponding to the transitions of the measured absorption spectra and free state of Dy^{3+} ions respectively. The bonding parameters (δ%) is dependent on (β) and is calculated with the help of this formula:

$$\delta = \frac{1 - \bar{\beta}}{\bar{\beta}} \tag{4}$$

where, $\bar{\beta}$ is the mean value of β. The bonding nature of ligands around the RE ions is dependent on positive or negative values for δ. In Table 2, it was observed that δ has positive values, which represent covalent bonding is prominent in these glasses.

The experimental oscillator strength (f_{exp}) is a key parameter, which was used to know the radiative properties of BaZnLiP glasses. The value of f_{exp} was calculated through the area of absorption peaks using the following equation [34–36].

$$f_{exp} = 4.318 \times 10^{-9} \int \in (\vartheta) d\vartheta \tag{5}$$

where $\in (\vartheta)$ is molar extinction coefficient for wave number ϑ cm^{-1} and calculated radiative parameters are listed in Table 2. J-O theory is employed to compute the intensity parameters (Ω_2, Ω_4, Ω_6) through a method of least-squares fit, as per the formula given in the literature [35]. To measure the quality fit between f_{exp} & f_{cal}, the rms deviation indicated by δ_{rms} can be estimated using the following formula:

$$\delta_{rms} = \left[\frac{\left(\sum (f_{exp} - f_{cal})^2 \right)}{N} \right]^{1/2} \tag{6}$$

where 'N' denotes the total number of peaks involved in fitting. Computed values of f_{exp}, f_{cal} and δ_{rms} were tabulated in Table 2.

Table 3
Judd-Ofelt parameters ($\Omega_t \times 10^{-20}$cm^2) of Dy^{3+} ions in BaZnLiP glasses along with various reported host glasses.

Glass System	Ω_2	Ω_4	Ω_6	Trend	References
PDY1	10.63	0.89	0.069	$\Omega_2 > \Omega_4 > \Omega_6$	Present work
PDY2	11.24	1.18	0.27	$\Omega_2 > \Omega_4 > \Omega_6$	Present work
PDY3	12.24	1.30	0.46	$\Omega_2 > \Omega_4 > \Omega_6$	Present work
PDY4	12.87	1.83	0.53	$\Omega_2 > \Omega_4 > \Omega_6$	Present work
PDY5	11.76	1.63	0.40	$\Omega_2 > \Omega_4 > \Omega_6$	Present work
Lead borosilicate	11.43	4.36	3.82	$\Omega_2 > \Omega_4 > \Omega_6$	[32]
SKNPLDy1.0 (PW)	10.02	4.84	2.70	$\Omega_2 > \Omega_4 > \Omega_6$	[14]
PZDy1.0	7.30	1.14	0.86	$\Omega_2 > \Omega_4 > \Omega_6$	[33]
KPKlCaFDy	13.30	3.38	2.83	$\Omega_2 > \Omega_4 > \Omega_6$	[34]
TeWLiK	12.70	6.202	1.827	$\Omega_2 > \Omega_4 > \Omega_6$	[35]

Table 4
Transition probability (A_R) (s^{-1}), luminescence branching ratio (β_R), total transition probability (A_T) (s^{-1}) and radiative lifetime (τ_R) (μs) for the observed emission transitions of Dy^{3+} ions in BaZnLiP glass.

Sample name	Transition	A_R	A_T	β_R	τ_R
PDY1	$^4F_{9/2} \rightarrow {}^6H_{11/2}$	16.49	1094.61	0.0151	913
	$^4F_{9/2} \rightarrow {}^6H_{13/2}$	824.28		0.7530	
	$^4F_{9/2} \rightarrow {}^6H_{15/2}$	109.91		0.1004	
PDY2	$^4F_{9/2} \rightarrow {}^6H_{11/2}$	36.02	1202.90	0.0299	831
	$^4F_{9/2} \rightarrow {}^6H_{13/2}$	896.93		0.7456	
	$^4F_{9/2} \rightarrow {}^6H_{15/2}$	116.89		0.0972	
PDY3	$^4F_{9/2} \rightarrow {}^6H_{11/2}$	52.30	1332.17	0.0393	750
	$^4F_{9/2} \rightarrow {}^6H_{13/2}$	991.13		0.7440	
	$^4F_{9/2} \rightarrow {}^6H_{15/2}$	126.79		0.0952	
PDY4	$^4F_{9/2} \rightarrow {}^6H_{11/2}$	64.15	1428.17	0.0449	700
	$^4F_{9/2} \rightarrow {}^6H_{13/2}$	1057.46		0.7404	
	$^4F_{9/2} \rightarrow {}^6H_{15/2}$	133.65		0.0936	
PDY5	$^4F_{9/2} \rightarrow {}^6H_{11/2}$	51.99	1297.93	0.0401	770
	$^4F_{9/2} \rightarrow {}^6H_{13/2}$	959.92		0.7396	
	$^4F_{9/2} \rightarrow {}^6H_{15/2}$	123.00		0.0948	

Comparatively less value of δ_{rms} is attained to justify the J-O theory in calculating J-O parameters and to know radiative properties of BaZnLiP glasses. The J-O parameters (Ω_2, Ω4, Ω6) were computed by the method of least squares fit and were represented in Table 3 and compared with other glasses reported in literature [15,36–44]. Intensity parameters imitate a similar trend ($\Omega_2 > \Omega_4 > \Omega_6$) for BaZnLiP glasses as given in the literature for other glasses [45–51]. The intensity parameter (Ω_2) presents the highest value for all BaZnLiP glasses, which represents covalent character for metal-ligand and asymmetric of BaZnLiP ions near Dy^{3+} ions. For BaZnLiP glasses intensity of transition $^6H_{15/2}$ to $^6F_{11/2} + {}^6H_{9/2}$

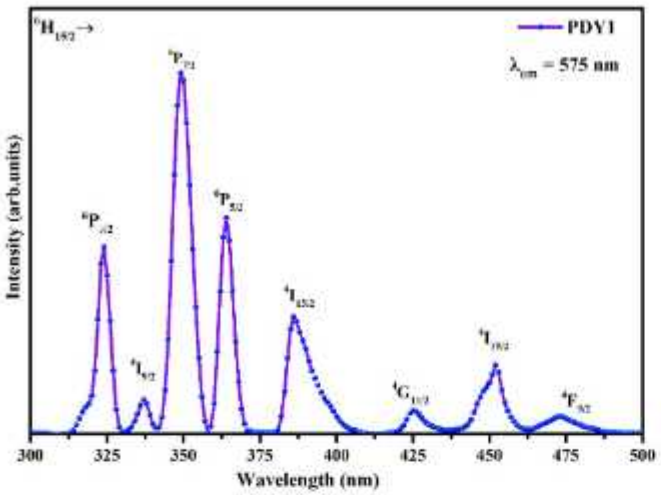

Fig. 7. Excitation spectrum of 1.0 mol% of Dy^{3+} ions in BaZnLiP glasses under 575 nm emission wavelength.

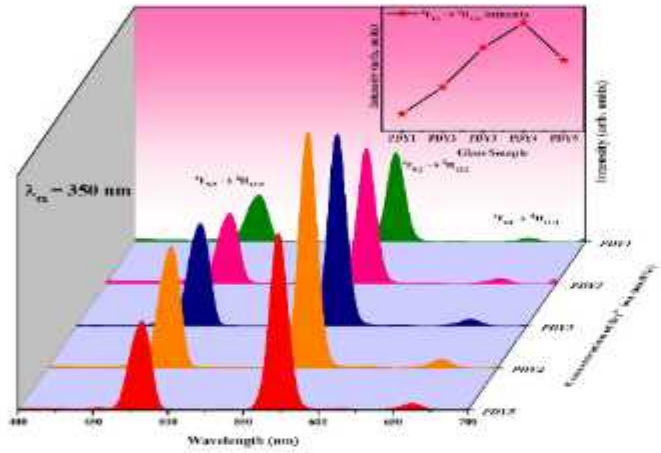

Fig. 8. Emission spectra of Dy^{3+} ions in BaZnLiP glasses monitored at 350 nm excitation wavelength. The inset plot shows the relative intensity variation of a most intense peak with different Dy-doped BaZnLiP glasses.

increases as Ω_2 increases, and vice versa. The prepared glasses show a value of Ω_2 rises from PDY1 to PDY4 glasses and drops for PDY5 glass. Among various prepared glasses, PDY4 glass has highest intensity for the hypersensitive transition and the lowest for PDY5 glass, which represents a higher symmetrical crystal structure of Dy^{3+} ions for PDY4 glass. Radiative parameters were calculated from intensity parameters such as A_R (radiative probability), β_R (luminescence branching ratio), τ_R (radiative lifetimes) as tabulated in Table 4. Required expressions for evaluating radiative properties were used from published literature [52].

3.5. PL excitation, PL emission and radiative properties analysis

PL properties of Dy^{3+} ion activated BaZnLiP glasses have been recorded at room temperature. The recorded PL excitation spectrum recorded for PDY3 glass (1% mol Dy^{3+} ions) exhibits several peaks in the range of 300–500 nm via monitoring the emission wavelength at 575 nm as illustrated in Fig. 7. The spectrum consists of several excitation peaks at wavelength 322, 337, 350, 362, 386, 425, 449, and 473 nm, which arises due to the transition from the lower energy level ($^6H_{15/2}$) to several higher energy states $^6P_{3/2}$, $^4I_{9/2}$, $^6P_{7/2}$, $^6P_{5/2}$, $^4I_{13/2}$, $^4G_{11/2}$, $^4H_{15/2}$ and $^4F_{9/2}$, of Dy^{3+} ions, respectively. The dominant transition was noticed at wavelength 350 nm, which is opted for recording the PL emission spectra for Dy^{3+} ions activated BZLP glasses.

The emission spectra recorded for Dy^{3+} ions activated BaZnLiP glasses at an excitation wavelength of 350 nm were depicted in Fig. 8. The PL spectra for all doped glasses have shown three peaks at 483, 575, and 663 nm due to transition from higher energy state $^4F_{9/2}$ to lower energy states at $^6H_{15/2}$, $^6H_{13/2}$, and $^6H_{11/2}$, respectively. Amid these PL peaks, transition ($^4F_{9/2} \rightarrow {}^6H_{13/2}$) was the most prominent as compared with the other two transitions. The intense transition ($^4F_{9/2} \rightarrow {}^6H_{13/2}$) was electric dipole in nature, extremely affected by nearby Dy^{3+} ions, and followed selection rule $\Delta L = \pm 2$, $\Delta S = 0$, $\Delta J = 0$ or ± 2. The ($^4F_{9/2} \rightarrow {}^6H_{15/2}$) transition was magnetic dipole (MD) in nature, which follows $\Delta J = 0$ or ± 1 selection rules & insensitive to the glass host environment. The yellow to blue (Y/B) intensity ratio is used to measure the rate of deformation in the glass matrix surrounded by Dy^{3+} ions and is also known as the asymmetry ratio. The ratio between yellow and blue PL peaks has been utilized as a tool to observe the configuration of radiant glass. The asymmetry ratio of RE i.e. (Dy^{3+}) ions change with the configuration of glass. The Y/B ratio is calculated for all the prepared glasses with the help of PL spectra and is tabulated in Table 6. In the present studies, the Y/B ratio for all prepared glasses is greater than 1. From the inset plot of Fig. 8, it can be perceived that the intensity of emission spectra gradually rises from PDY1 to PDY4 glass as the concentration changes from 0.1 to 1.5 mol% of Dy^{3+} ions and reduces for PDY5 glass. This decrement in intensity beyond 1.5 mol% of the doped ion is due to concentration quenching that took place by resonant energy transfer (RET) and mutual interactions between Dy^{3+}- Dy^{3+} ions that describes the self-quenching mechanism [53].

An energy level diagram depicted in Fig. 9 explains all processes such as excitation, emission, RET, and CR channels. Due to the small energy gap in the higher excited states above $^4F_{9/2}$, the non-radiative transitions take place and are therefore known as radiation-less relaxation energy levels. Such non-radiative relaxations ultimately populate the $^4F_{9/2}$ energy state and consequently, radiative emissions start occurring from the $^4F_{9/2}$ energy state to $^6H_{15/2}$,$H_{13/2}$ and $^6H_{11/2}$ lower levels producing intense peaks at the blue, yellow, and red color of the visible spectrum, respectively. The energy gap between $^4F_{9/2}$ and $^6F_{3/2}$ is sufficiently large (~6600 cm^{-1}) than the phonon energy of the host glass (~1300 cm^{-1}), and this leads to achieving intense luminous radiative transitions as shown in Fig. 9 [54]. Fig. 9 also depicted the resonance energy transfer ($^4F_{9/2}+{}^6H_{15/2} \leftrightarrow {}^6H_{15/2}+{}^4F_{9/2}$) and possible cross-relaxation channels, CRC-1, CRC-2, and CRC-3 for as prepared glasses [38,55–58].

To understand more about the utility of the titled glasses for laser and optoelectronic device applications, the PL spectra for Dy^{3+} doped BaZnLiP glasses have been further used to estimate some radiative parameters like luminescence branching ratio (β_R), radiative transition probability (A_R), total transition probability (A_T) and radiative lifetime (τ_R) using relevant formulas that are given in the literature [59]. Stimulated emission cross-section (σ_{se}) is an important parameter used to know more about the lasing potentiality of a host matrix can be calculated by employing the following formula:

$$\sigma_{se} = \frac{\lambda_p^4}{8\pi c n^2 \Delta\lambda_p} A_R \quad (7)$$

where λ_p denotes the wavelength of PL peak, $\Delta\lambda_p$ denotes effective bandwidth, A_R denotes transition probability, c and n are the velocity of light and refractive index, respectively. Radiative parameters A_R, β_R, and A_T calculated for Dy^{3+} doped BaZnLiP glasses are tabulated in Table 4. Branching ratio is another crucial parameter for the designing of a laser. The higher value of $\beta_R > 0.5$ specifies the probability of achieving a more stimulated emission for a particular transition. An important parameter was the high value of stimulated cross-section for obtaining high gain and identifying laser transitions of Dy^{3+} ions in host glass for various CW laser applications. Moreover, higher values of σ_{se} x $\Delta\lambda p$ (gain bandwidth) and σ_{se} x τ_R (optical gain parameters) have characteristics of good optical fiber and were listed in Table 5. The value of σ_{se} and β_R

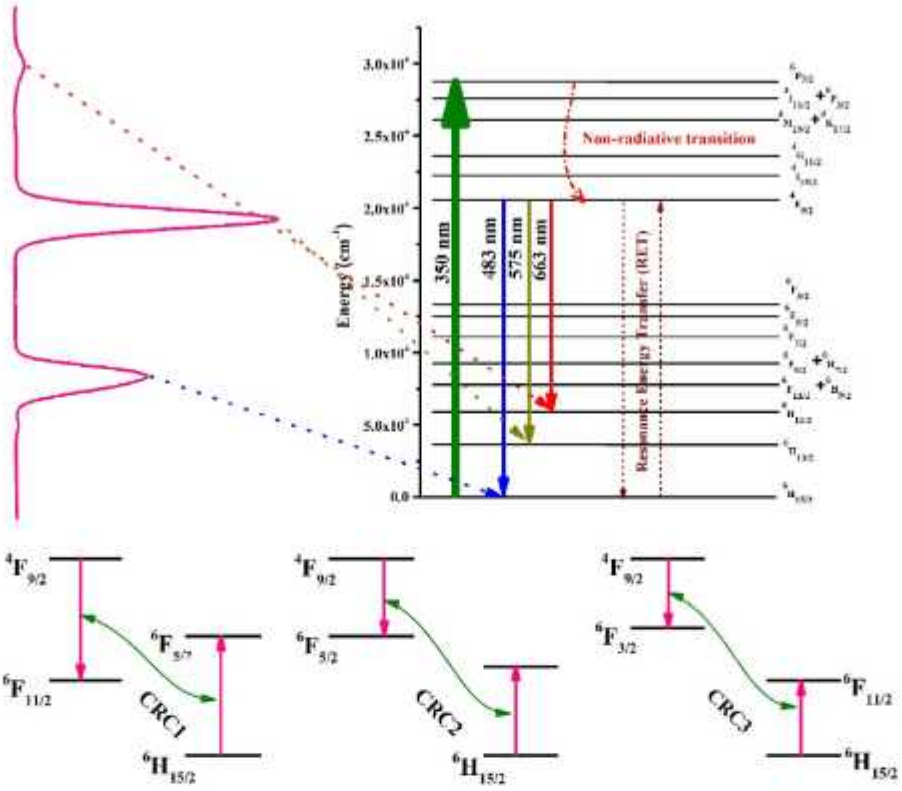

Fig. 9. Partial energy level diagram showing absorption, excitation, emission and cross-relaxation mechanism for Dy^{3+} ions in BaZnLiP glasses.

Table 5
Emission peak wavelength (λ_P)(nm), effective bandwidths ($\Delta\lambda_P$) (nm), measured and experimental branching ratios (β_R &β_{exp}), stimulated emission cross-sections (σ_{se}) (cm^2), gain bandwidth ($\sigma_{se} \times \Delta\lambda_P$) ($cm^2$) and optical gain parameter ($\sigma_{se} \times \tau_R$) ($cm^2$ s) parameters for the emission transitions for Dy^{3+} ions in BaZnLiP glasses.

Spectral parameters	PDY1	PDY2	PDY3	PDY4	PDY5
$^4F_{9/2} \rightarrow {}^6H_{15/2}$					
λ_P	663	663	663	663	663
$\Delta\lambda_P$	14.53	15.16	15.29	15.45	15.93
β_R	0.01	0.02	0.03	0.04	0.04
β_{exp}	0.02	0.02	0.02	0.02	0.02
σ_{se}	1.13	2.37	3.42	4.15	3.26
$\sigma_{se} \times \Delta\lambda_P$	1.65	3.60	5.23	6.42	5.20
$\sigma_{se} \times \tau_R$	1.03	1.97	2.56	2.91	2.51
$^4F_{9/2} \rightarrow {}^6H_{13/2}$					
λ_P	575	575	575	575	575
$\Delta\lambda_P$	13.22	13.18	13.33	13.36	13.37
β_R	0.75	0.74	0.74	0.74	0.73
β_{exp}	0.56	0.56	0.59	0.60	0.59
σ_{se}	35.32	38.53	42.10	44.84	40.66
$\sigma_{se} \times \Delta\lambda_P$	46.70	50.82	56.15	59.92	54.39
$\sigma_{se} \times \tau_R$	32.24	32.02	31.56	31.39	31.31
$^4F_{9/2} \rightarrow {}^6H_{11/2}$					
λ_P	483	483	483	483	483
$\Delta\lambda_P$	12.90	11.67	12.05	11.90	11.97
β_R	0.10	0.09	0.09	0.09	0.09
β_{exp}	0.35	0.35	0.36	0.34	0.34
σ_{se}	2.51	2.62	2.96	3.16	2.89
$\sigma_{se} \times \Delta\lambda_P$	3.10	3.29	3.57	3.77	3.47
$\sigma_{se} \times \tau_R$	2.90	2.94	2.22	2.21	2.23

were highest for PDY4 glass related to $^4F_{9/2} \rightarrow {}^6H_{13/2}$ transition and similar to other reported values [60,61]. Further, it is observed that various radiative parameters as mentioned above have the highest values for PDY4 glass for its relatively intense transition $^4F_{9/2} \rightarrow {}^6H_{13/2}$, which makes this glass suitable in solid-state lighting and lasing applications.

Table 6
Experimental lifetime (τ_{exp}) (μs), radiative lifetime (τ_R) (μs), quantum efficiency (η), Y/B ratio and non-radiative decay rates (W_{NR}) (s^{-1}), for Dy^{3+} ions in BaZnLiP glasses.

Sample	τ_{exp} (μs)	τ_R (μs)	η (%)	Y/B	W_{NR}
PDY1	584	913	63	1.73	617
PDY2	565	831	67	1.69	566
PDY3	555	750	74	1.80	468
PDY4	536	700	77	1.96	437
PDY5	489	770	63	1.92	746

Table 7
CIE coordinates of Dy^{3+} ions in BaZnLiP glasses.

Name of the sample	CIE co-ordinates		CCT(K)
	X co-ordinate	Y co-ordinate	
PDY1	0.354	0.412	4609
PDY2	0.356	0.40	4588
PDY3	0.361	0.394	4525
PDY4	0.362	0.391	4474
PDY5	0.372	0.414	4453

3.6. Colorimetric properties

The Commission International de l'Eclairage (CIE) coordinates were evaluated for Dy^{3+} activated BaZnLiP glasses using PL spectra under wavelength 350 nm. CIE coordinates for PDY1 to PDY5 BaZnLiP glasses were tabulated in Table 7. The CIE coordinates for optimizing glass i.e., PDY4 glass is (0.362, 0.391) as indicated in Fig. 10, which is placed in a white zone and nearby with a standard white light point (0.33, 0.33). One of the important parameters known as correlated color

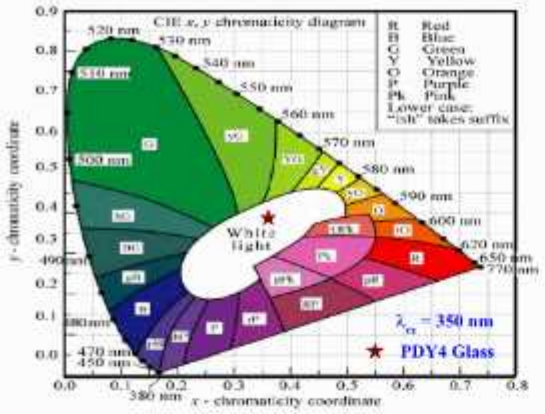

Fig. 10. CIE chromaticity coordinates of 1.5 mol% Dy^{3+} ions in BaZnLiP glass.

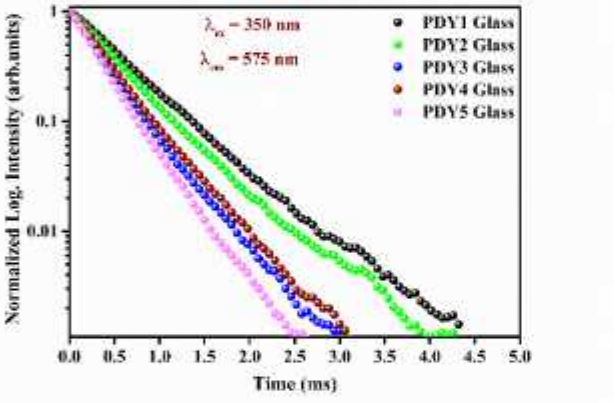

Fig. 11. Decay profile of Dy^{3+} ions in BaZnLiP glasses for $^4F_{9/2} \rightarrow {}^6H_{13/2}$ (575 nm) transition under 350 nm excitation wavelength.

temperatures (CCT) is used to get familiar with the trait of emission. Moreover, it is specified as a black body Planckian radiator temperature, the color emitted by the Planckian radiator is nearly similar to the color emitted by the white light source. CCT is evaluated using the McCamy formula with the help of chromaticity coordinates in this manner:

$$CCT = -449\ n^3 + 3525\ n^2 - 6823.3n + 5520.33 \quad (8)$$

where, $n = \frac{(x - x_e)}{(y - y_e)}$ is inverse slope line and (x_e, y_e) (= 0.332, 0.186) is epicenter [62,63]. CCT values were evaluated for differing concentrations of Dy^{3+} doped BaZnLiP glasses and represented in Table 7. The calculated values are observed in the range 4000K–5000K specifically lie in the bright white region, which makes them reliable for visible lasers and lighting applications.

3.7. PL decay spectral analysis

The PL radiative decay curves for highly intense peak $^4F_{9/2} \rightarrow {}^6H_{13/2}$ observed at 575 nm emission under 350 nm excitation were shown in Fig. 11. For the different concentrations of Dy^{3+} ions, the PL decay profile curves are recognized as exponential in nature. The experimental lifetimes (τ_{exp}) for all the as-prepared glasses were estimated by using the observed PL decay curves and tabulated in Table 6 along with radiative lifetime (τ_R) values. From Table 6, it has been noticed that the

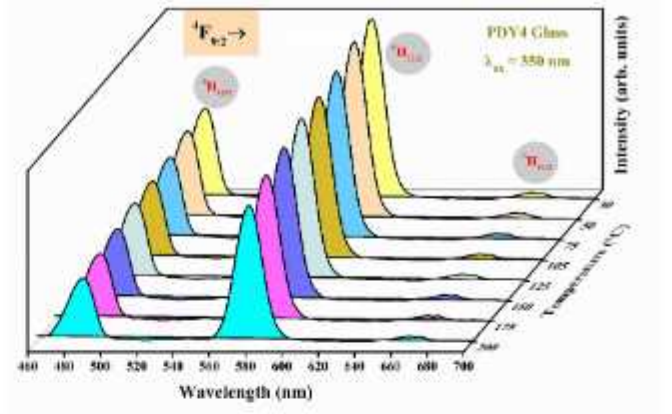

Fig. 12. Temperature-dependent PL spectra for 1.5 mol% Dy^{3+} ions in BaZnLiP glass.

τ_{exp} values are smaller than τ_R. The variation in the observed data arises because of phonon energy transfer by the donors and interlinked between Dy^{3+} ions with OH vibrational bands available in prepared glasses [64]. One more important parameter useful in understanding the lasing potentiality of the as-prepared glasses is quantum efficiency (η), which is defined as the ratio of output photons to input photons. Practically such η value can be evaluated for the glasses under study by using the following expression:

$$\eta = \frac{\tau_{exp}}{\tau_R} \quad (9)$$

The calculated values of η for all the titled glasses are given in Table 6. From the data appearing in Table 6, it is conspicuous that among all the glasses investigated in the present work, PDY4 glass is best suited for lasing action at 575 nm as it has a relatively high η value in comparison with other glasses. The non-radiative energy transfer (W_{NR}) can be calculated by using the following formula:

$$W_{NR} = \frac{1}{\tau_{exp}} - \frac{1}{\tau_R} \quad (10)$$

The estimated W_{NR} values for the titled glasses are depicted in Table 6. Among all the titled glasses, PDY4 glass perceives relatively least W_{NR} value indicating its superiority in achieving more radiative emissions that other glasses. Glasses having relatively less W_{NR} values are more liable and prone to show high stimulated cross-section and quantum efficiency, which are essential for getting potential lasing action.

3.8. Temperature dependent photoluminescence (TD-PL) studies

In the process of understanding the thermal stability of the optimized glass (PDY4), the TD-PL spectra have been recorded for it 575 nm under λ_{ex} = 350 nm and are shown in Fig. 12. The data plotted in Fig. 12 reveals that the PL intensity of Dy^{3+} ions in PDY4 glass is diminishing as the temperature rises from room temperature (27 °C) to 200 °C. The PL intensity of all the peaks was reduced due to the thermal quenching of the luminescent characteristics. A clear analysis of the data shown in Fig. 12 allows us to contemplate that PDY4 glass at 150 °C retains 85.34% of its intensity in comparison to its initial intensity. Further, this value fall down to 75.49% at 200 °C. This data obtained from TD-PL spectra reveals that the optimized glass is having relatively high thermal stability. Furthermore, the activation energy (ΔE_a) for the optimized glass has been evaluated using the expression given by the Arrhenius equation [65]:

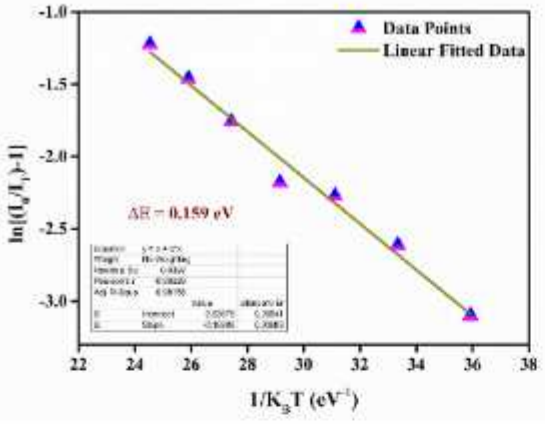

Fig. 13. Graph between $\ln[(I_o/I_T)-1]$ and $(1/K_BT)$ for 1.5 mol% Dy^{3+} ions in BaZnLiP glass.

$$I_T = \frac{I_0}{1 + C\,exp\left(-\frac{\Delta E}{K_B T}\right)} \tag{11}$$

as per the expression I_0 and I_T indicate the PL intensity at room temperature and T (K) temperature, respectively. C signifies a constant and K_B signifies the Boltzmann constant. The linearly fitted graph between ln $((I_0/I_T)-1)$ with $1/K_BT$ plot gives the slope value, which is equal to the activation energy for the prepared glass as presented in Fig. 13. The ΔE value is found to be 0.159 eV for PDY4 glass which is less than the value already reported literature [66]. Thus, the TD-PL spectral data obtained for PDY4 glass showcases its superior nature in exhibiting excellent thermal stability.

4. Conclusions

BaZnLiP glasses with varying Dy^{3+} ions concentrations were prepared via melt quenching routes and studied their numerous spectroscopic characteristics to know their applicability in the visible photonic device applications. The non-crystalline nature of the undoped BaZnLiP glass is confirmed by the XRD pattern. From the FT-IR spectral recording, several vibration bands were noticed in the as-prepared undoped BaZnLiP glass and confirms the formation of various bonds. Dy^{3+} activated BaZnLiP glasses are effectively absorbing UV, visible, and NIR radiation having an optical bandgap in the 3.64–3.76 eV range. Radiative properties of distinguished glowing levels of Dy^{3+} ions in BaZnLiP glasses were measured through J–O parameters. The PL spectra of BaZnLiP glasses reveal three sharp peaks, out of which yellow emission (575 nm) was the more intense as compared with blue, and red emission under 350 nm excitation wavelength. The decay curves show the exponential in nature. The calculated CIE coordinates are in good approximation with standard white light points (0.33, 0.33) of equal energy and lie in the visible region. The values of CCT of BaZnLiP glasses fall in the bright white light and make them suitable for w-LEDs. Relatively high activation energy obtained for PDY4 glass from the recorded TD-PL spectrum reveals excellent thermal stability for it. From the various calculated radiative parameters especially quantum efficiency and stimulated emission cross-section, it was summarized that among various Dy^{3+} activated BaZnLiP glasses, PDY4 glass (BaZnLiP glass with 1.5 mol% of Dy^{3+} ion concentration) is quite suitable for the fabrication of visible photonic devices such as yellow lasers and w-LEDs.

CRediT authorship contribution statement

Kartika Maheshwari: Ms. . **A.S. Rao:** work plan, experiments, calculation and writing the manuscript, Prof. .

Declaration of competing interest

The authors declare that they have no known competing financial interests or personal relationships that could have appeared to influence the work reported in this paper.

Acknowledgement

The authors are thankful to the authorities of DTU for providing the necessary infrastructure facilities to carryout the present work.

References

[1] A.A. Reddy, M.C. Sekhar, K. Pradeesh, S.S. Babu, G.V. Prakash, Optical properties of Dy^{3+}-doped sodium-aluminum-phosphate glasses, J. Mater. Sci. 46 (2011) 2018–2023, https://doi.org/10.1007/s10853-010-4851-3.

[2] S. Selvi, G. Venkataiah, S. Arunkumar, G. Muralidharan, K. Marimuthu, Structural and luminescence studies on Dy^{3+} doped lead boro-telluro-phosphate glasses, Phys. B Condens. Matter 454 (2014) 72–81, https://doi.org/10.1016/j.physb.2014.07.018.

[3] Y.N.C. Ravi Babu, P. Sree Ram Naik, K. Vijaya Kumar, N. Rajesh Kumar, A. Suresh Kumar, Spectral investigations of Sm^{3+} doped lead bismuth magnesium borophosphate glasses, J. Quant. Spectrosc. Radiat. Transf. 113 (2012) 1669–1675, https://doi.org/10.1016/j.jqsrt.2012.03.034.

[4] A. Srinivasa Rao, B. Rupa Venkateswara Rao, M.V.V.K.S. Prasad, J.V. Shanmukha Kumar, M. Jayasimhadri, J.L. Rao, R.P.S. Chakradhar, Spectroscopic and optical properties of Nd^{3+} doped fluorine containing alkali and alkaline earth zinc-aluminophosphate optical glasses, Phys. B Condens. Matter 404 (2009) 3717–3721, https://doi.org/10.1016/j.physb.2009.06.114.

[5] A.S. Rao, Y.N. Ahammed, R.R. Reddy, T.V.R. Rao, Spectroscopic Studies of Nd^{3+}-doped Alkali Fluoroborophosphate Glasses. Optical Materials 10, Elsevier, 1998, pp. 245–252.

[6] Y. Tayal, A.S. Rao, Orange color emitting Sm^{3+} ions doped borosilicate glasses for optoelectronic device applications, Opt. Mater. (Amst). 107 (2020), https://doi.org/10.1016/j.optmat.2020.110070.

[7] Y.G. Choi, J. Heo, 3 Tm Emission and Multiphonon Relaxation Phenomena in $PbO-Bi_2O_3-Ga_2O_3$ Glasses Doped with Rare-Earths, 1997.

[8] J.S. Kim, K.T. Lim, Y.S. Jeong, P.E. Jeon, J.C. Choi, H.L. Park, Full-color $Ba_3MgSi_2O_8:Eu^{2+}$, Mn^{2+} phosphors for white-light-emitting diodes, Solid State Commun. 135 (2005) 21–24, https://doi.org/10.1016/j.ssc.2005.03.068.

[9] C. Zhu, Y. Yang, X. Liang, S. Yuan, G. Chen, Rare earth ions doped full-color luminescence glasses for white LED, J. Lumin. 126 (2007) 707–710, https://doi.org/10.1016/j.jlumin.2006.10.028.

[10] H. Masai, Y. Yamada, Y. Suzuki, K. Teramura, Y. Kanemitsu, T. Yoko, Narrow energy gap between triplet and singlet excited states of Sn^{2+} in borate glass, Sci. Rep. 3 (2013), https://doi.org/10.1038/srep03541.

[11] K. Jha, M. Jayasimhadri, Spectroscopic investigation on thermally stable Dy^{3+}doped zinc phosphate glasses for white light emitting diodes, J. Alloys Compd. 688 (2016) 833–840, https://doi.org/10.1016/j.jallcom.2016.07.024.

[12] R.J. Amjad, M.R. Dousti, M.R. Sahar, Spectroscopic investigation and Judd-Ofelt analysis of silver nanoparticles embedded Er^{3+}-doped tellurite glass, Curr. Appl. Phys. 15 (2015) 1–7, https://doi.org/10.1016/j.cap.2014.10.022.

[13] M. Higuchi, R. Sasaki, J. Takahashi, Float zone growth of Dy:$GdVO_4$ single crystals for potential use in solid-state yellow lasers, J. Cryst. Growth 311 (2009) 4549–4552, https://doi.org/10.1016/j.jcrysgro.2009.08.028.

[14] Z. Yan, X. Zhongxi, L. Chunhua, &-Q), N. Yan, Z. Qiu, Optical Properties of Dy^{3+}Doped in Boroaluminasilicate Glass. Journal of Rare Earths 25, Elsevier, 2007, p. 99.

[15] P. Manasa, C.K. Jayasankar, Spectroscopic assessment of Dy^{3+} ions in lead fluorosilicate glass as a prospective material for solid state yellow laser, Spectrochim. Acta Part A Mol. Biomol. Spectrosc. 212 (2019) 315–321, https://doi.org/10.1016/j.saa.2019.01.015.

[16] Y.H. Zhang, D.S. Li, X. Zhao, E.Y.B. Pun, H. Lin, Photon releasing of Dy^{3+} doped fluoroborate glasses for laser illumination, J. Alloys Compd. 728 (2017) 1279–1288, https://doi.org/10.1016/j.jallcom.2017.09.108.

[17] C. Madhukar Reddy, G.R. Dillip, B. Deva Prasad Raju, Spectroscopic and photoluminescence characteristics of Dy^{3+} ions in lead containing sodium fluoroborate glasses for laser materials, J. Phys. Chem. Solid. 72 (2011) 1436–1441, https://doi.org/10.1016/j.jpcs.2011.08.023.

[18] A.M. Babu, B.C. Jamalaiah, J.S. Kumar, T. Sasikala, L.R. Moorthy, Spectroscopic and photoluminescence properties of Dy^{3+}-doped lead tungsten tellurite glasses for laser materials, J. Alloys Compd. 509 (2011) 457–462, https://doi.org/10.1016/j.jallcom.2010.09.058.

[19] I. Khan, G. Rooh, R. Rajaramakrishna, N. Srisittipokakun, C. Wongdeeying, N. Kiwwakunkran, N. Wantana, H.J. Kim, J. Kaewkhao, S. Tuscharoen, Photoluminescence and white light generation of Dy_2O_3 doped $Li_2O-BaO-Gd_2O_3-SiO_2$ for white light LED, J. Alloys Compd. 774 (2019) 244–254, https://doi.org/10.1016/j.jallcom.2018.09.156.

[20] P. Rekha Rani, M. Venkateswarlu, S. Mahamuda, K. Swapna, N. Deopa, A.S. Rao, Spectroscopic studies of Dy^{3+} ions doped barium lead alumino fluoro borate glasses, J. Alloys Compd. 787 (2019) 503–516, https://doi.org/10.1016/j.jallcom.2019.02.088.

[21] S. Tian, Y. Lun, Y. Sun, D. Chen, G. Tang, Q. Qian, Z. Yang, Silicate-clad Dy^{3+} doped multi-component phosphate glass core glass fiber for yellow laser applications, J. Non-Cryst. Solids (2021) 121313, https://doi.org/10.1016/j.jnoncrysol.2021.121313.

[22] P. Babu, V. Chandrappa, N. Vijaya, C.K. Jayasankar, H.J. Seo, Optical and white light emission properties of Dy^{3+} ions doped zinc oxyfluorotellurite glasses, Phys. B Condens. Matter 614 (2021) 413037, https://doi.org/10.1016/j.physb.2021.413037.

[23] R.J. Amjad, T.O. Sales, A. Sattar, C. Jacinto, M.R. Dousti, Spectral studies of highly Dy^{3+} doped PbO–ZnO–B_2O_3–P_2O_5 glasses, J. Lumin. 231 (2021) 117839, https://doi.org/10.1016/j.jlumin.2020.117839.

[24] R.S. Gedam, D.D. Ramteke, Effect of Sm_2O_3 addition on electrical and optical properties of lithium borate glasses, AIP Conf. Proc. (2012) 561–562, https://doi.org/10.1063/1.4710127.

[25] W.T. Carnall, P.R. Fields, K. Rajnak, Electronic energy levels of the trivalent lanthanide aquo ions. I. Pr3+, Nd3+, Pm3+, Sm3+,Dy3+, Ho3+, Er3+ and Tm3+, J. Chem. Phys. 49 (1968) 4424–4442, https://doi.org/10.1063/1.1669893.

[26] A.H. Khafagy, M.A. Ewaida, A.A. Higazy, M.M. S Ghoneim, I.Z. Hager, R. El-bahnasawy, Infrared Spectra and Composition Dependence Investigations of the Vitreous V2O5/P2O5 System. J. Mater.Sci. 27, Springer, 1992, pp. 1435–1439.

[27] R. Lakshmikantha, R. Rajaramakrishna, R.V. Anavekar, N.H. Ayachit, Characterization and structural studies of lithium doped lead zinc phosphate glass system, Mater. Chem. Phys. 133 (2012) 249–252, https://doi.org/10.1016/j.matchemphys.2012.01.017.

[28] Y.B. Saddeek, Network structure of molybdenum lead phosphate glasses: infrared spectra and constants of elasticity, Phys. B Condens. Matter 406 (2011) 562–566, https://doi.org/10.1016/j.physb.2010.11.041.

[29] A.M. E®mov, V.G. Pogareva, Water-related IR absorption spectra for some phosphate and silicate glasses, n.d. www.elsevier.com/locate/jnoncrysol.

[30] M. Kumar, A.S. Rao, Concentration-dependent reddish-orange photoluminescence studies of Sm^{3+} ions in borosilicate glasses, Opt. Mater. (Amst). 109 (2020) 110356, https://doi.org/10.1016/j.optmat.2020.110356.

[31] E. Mansour, G. El-Damrawi, Electrical properties and FTIR spectra of ZnO-PbO-P_2O_5 glasses, Phys. B Condens. Matter 405 (2010) 2137–2143, https://doi.org/10.1016/j.physb.2010.01.121.

[32] M. Altaf, M.A. Chaudhry, M. Zahid, STUDY OF OPTICAL BAND GAP OF ZINC-BORATE GLASSES 14 (2003) 253–259.

[33] C. Klixbull Jørgensen, The nephelauxetic series, Prog.Inorg.chem 4 (1962) 73.

[34] B.R. Judd, Optical absorption intensities of rare-earth ions, Phys. Rev. 127 (1962) 750–761, https://doi.org/10.1103/PhysRev.127.750.

[35] N. Deopa, A.S. Rao, Photoluminescence and energy transfer studies of Dy^{3+} ions doped lithium lead alumino borate glasses for w-LED and laser applications, J. Lumin. 192 (2017) 832–841, https://doi.org/10.1016/j.jlumin.2017.07.052.

[36] M. Reddi Babu, N. Madhusudhana Rao, A. Mohan Babu, N. Jaidass, C. Krishna Moorthy, L. Rama Moorthy, Effect of Dy^{3+} ions concentration on optical properties of lead borosilicate glasses for white light emission, Optik (Stuttg). 127 (2016) 3121–3126, https://doi.org/10.1016/j.ijleo.2015.12.018.

[37] A. Lira, A. Speghini, E. Camarillo, M. Bettinelli, U. Caldiño, Spectroscopic evaluation of Zn $(PO_3)_2$: Dy^{3+} glass as an active medium for solid state yellow laser, Opt. Mater. (Amst). 36 (2014) 188–192, https://doi.org/10.1016/j.optmat.2014.10.024.

[38] S.N. Rasool, L. Rama Moorthy, C.K. Jayasankar, Optical and luminescence properties of Dy^{3+} ions in phosphate based glasses, Solid State Sci. 22 (2013) 82–90, https://doi.org/10.1016/j.solidstatesciences.2013.05.013.

[39] C.B. Annapurna Devi, S. Mahamuda, M. Venkateswarlu, K. Swapna, A. Srinivasa Rao, G. Vijaya Prakash, Dy^{3+} ions doped single and mixed alkali fluoro tungsten tellurite glasses for LASER and white LED applications, Opt. Mater. (Amst). 62 (2016) 569–577, https://doi.org/10.1016/j.optmat.2016.11.016.

[40] K. Swapna, S. Mahamuda, A. Srinivasa Rao, M. Jayasimhadri, T. Sasikala, L. Rama Moorthy, Visible fluorescence characteristics of Dy^{3+} doped zinc alumino bismuth borate glasses for optoelectronic devices, Ceram. Int. 39 (2013) 8459–8465, https://doi.org/10.1016/j.ceramint.2013.04.028.

[41] Y.C. Ratnakaram, D. Thirupathi Naidu, A. Vijayakumar, J.L. Rao, Studies on optical absorption and luminescence properties of Dy^{3+} doped mixed alkali borate glasses, Opt. Mater. (Amst). 27 (2004) 409–417, https://doi.org/10.1016/j.optmat.2004.01.020.

[42] Y.B. Shin, J. Heo, Mid-infrared emissions and multiphonon relaxation in Dy^{3+}-doped chalcohalide glasses, n.d. www.elsevier.com/locate/jnoncrysol.

[43] R.R. Jacobs, M.J. Weber, Induced-emission cross sections for the $^4F_{3/2} \rightarrow {}^4I_{13/2}$ transition in neodymium laser glasses, IEEE J. Quant. Electron. 11 (1975) 846–847, https://doi.org/10.1109/JQE.1975.1068582.

[44] B.C. Jamalaiah, L.R. Moorthy, H.J. Seo, Effect of lead oxide on optical properties of Dy^{3+} ions in PbO-H_3BO_3-TiO_2-AlF_3 glasses, J. Non-Cryst. Solids 356 (2012) 204–209, https://doi.org/10.1016/j.jnoncrysol.2011.09.007.

[45] N. Luewarasirikul, H.J. Kim, P. Meejitpaisan, J. Kaewkhao, White light emission of dysprosium doped lanthanum calcium phosphate oxide and oxyfluoride glasses, Opt. Mater. (Amst). 66 (2017) 559–566, https://doi.org/10.1016/j.optmat.2017.02.049.

[46] M. Vijayakumar, K. Marimuthu, Structural and luminescence properties of Dy^{3+} doped oxyfluoro-borophosphate glasses for lasing materials and white LEDs, J. Alloys Compd. 629 (2015) 230–241, https://doi.org/10.1016/j.jallcom.2014.12.214.

[47] T.G.V.M. Rao, A. Rupesh Kumar, K. Neeraja, N. Veeraiah, M. Rami Reddy, Optical and structural investigation of Dy^{3+}-Nd^{3+} co-doped in magnesium lead borosilicate glasses, Spectrochim. Acta Part A Mol. Biomol. Spectrosc. 118 (2014) 744–751, https://doi.org/10.1016/j.saa.2013.09.061.

[48] T. Sasikala, L. Rama Moorthy, A. Mohan Babu, T. Srinivasa Rao, Effect of co-doping Tm^{3+} ions on the emission properties of Dy^{3+} ions in tellurite glasses, J. Solid State Chem. 203 (2013) 55–59, https://doi.org/10.1016/j.jssc.2013.03.056.

[49] V. Uma, K. Marimuthu, G. Muralidharan, Influence of modifier cations on the spectroscopic properties of Dy^{3+} doped telluroborate glasses for white light applications, J. Fluoresc. 26 (2016) 2281–2294, https://doi.org/10.1007/s10895-016-1924-y.

[50] K. Siva Rama Krishna Reddy, K. Swapna, S. Mahamuda, M. Venkateswarlu, A. S. Rao, G. Vijaya Prakash, Investigation on structural and luminescence features of Dy^{3+} ions doped alkaline-earth boro tellurite glasses for optoelectronic devices, Opt. Mater. (Amst). 85 (2018) 200–210, https://doi.org/10.1016/j.optmat.2018.08.057.

[51] S. Zulfiqar Ali Ahamed, C. Madhukar Reddy, B. Deva Prasad Raju, Structural, thermal and optical investigations of Dy^{3+} ions doped lead containing lithium fluoroborate glasses for simulation of white light, Opt. Mater. (Amst). 35 (2013) 1385–1394, https://doi.org/10.1016/j.optmat.2013.02.006.

[52] D.L. Dexter, J.H. Schulman, Theory of concentration quenching in inorganic phosphors, J. Chem. Phys. 22 (1954) 1063–1070, https://doi.org/10.1063/1.1740265.

[53] J. Pisarska, L. Zur, W.A. Pisarski, Structural and optical characterization of Dy-doped heavy-metal oxide and oxyhalide borate glasses, Phys. Status Solidi Appl. Mater. Sci. 209 (2012) 1134–1140, https://doi.org/10.1002/pssa.201127555.

[54] J. Suresh Kumar, K. Pavani, A. Mohan Babu, N. Kumar Giri, S.B. Rai, L.R. Moorthy, Fluorescence characteristics of Dy^{3+} ions in calcium fluoroborate glasses, J. Lumin. 130 (2010) 1916–1923, https://doi.org/10.1016/j.jlumin.2010.05.006.

[55] T. Srihari, C.K. Jayasankar, Fluorescence properties and white light generation from Dy^{3+}-doped niobium phosphate glasses, Opt. Mater. (Amst). 69 (2017) 87–95, https://doi.org/10.1016/j.optmat.2017.04.001.

[56] P. Karthikeyan, R. Vijayakumar, K. Marimuthu, Luminescence studies on Dy^{3+} doped calcium boro-tellurite glasses for White light applications, Phys. B Condens. Matter 521 (2017) 347–354, https://doi.org/10.1016/j.physb.2017.07.018.

[57] F. Zaman, J. Kaewkhao, N. Srisittipokakun, N. Wantana, H.J. Kim, G. Rooh, Investigation of luminescence and laser transition of Dy^{3+} in Li_2O-Gd_2O_3-Bi_2O_3-B_2O_3 glasses, Opt. Mater. (Amst). 55 (2016) 136–144, https://doi.org/10.1016/j.optmat.2016.03.024.

[58] R. Casesa, M.A. Chamarroa, R. Alcalaa, V.D. Rodriguesb, Optical Properties of $Nd^{3+}$and Dy^{3+} Ions in ZnF_2-CdF_2 Based Glasses. J. Lumin. 48 & 49, Elsevier, 1991, pp. 509–514.

[59] C. Venkateswarlu, M. Seshadri, Y.C. Ratnakaram, Influence of mixed alkalis on spectroscopic parameters of Sm^{3+}, Dy^{3+} doped chloroborate glasses, Opt. Mater. (Amst). 33 (2011) 799–806, https://doi.org/10.1016/j.optmat.2010.12.022.

[60] P. Babu, K.H. Jang, E.S. Kim, L. Shi, R. Vijaya, V. Lavín, C.K. Jayasankar, H.J. Seo, Optical properties and energy transfer of Dy^{3+}-doped transparent oxyfluoride glasses and glass-ceramics, J. Non-Cryst. Solids 356 (2010) 236–243, https://doi.org/10.1016/j.jnoncrysol.2009.11.010.

[61] R.D. Peacock, The intensities of lanthanide f ⟷ f transitions, Struct. Bond 22 (1975) 83–122.

[62] C.S. McCamy, Correlated color temperature as an explicit function of chromaticity coordinates, Color Res. Appl. 17 (1992) 142–144, https://doi.org/10.1002/col.5080170211.

[63] S. Kaur, A.K. Vishwakarma, N. Deopa, A. Prasad, M. Jayasimhadri, A.S. Rao, Spectroscopic studies of Dy^{3+} doped borate glasses for cool white light generation, Mater. Res. Bull. 104 (2018) 77–82, https://doi.org/10.1016/j.materresbull.2018.04.002.

[64] S. Arunkumar, G. Venkataiah, K. Marimuthu, Spectroscopic and energy transfer behaviour of Dy^{3+} ions in B_2O_3 -TeO$_2$ - PbO- PbF_2 - Bi_2O_3 - CdO glasses for laser AND WLED applications, Spectrochim, Acta- PartA Mol. Biomol. spectrosc. 136 (2015) 1684–1697, https://doi.org/10.1016/j.saa.2014.10.067.

[65] M.K. Sahu, J. Mula, White light emitting thermally stable bismuth phosphate phosphor $Ca_2Bi(PO_4)_2$:Dy^{3+} for solid-state lighting applications, J. Am. Ceram. Soc. 102 (2019) 6087–6099, https://doi.org/10.1111/jace.16479.

[66] A.S. Rao Ravita, Ravita, A.S. Rao, Effective energy transfer from Dy^{3+} to Tb^{3+} ions in thermally stable KZABS glasses for intense green emitting device applications, J. Lumin. 239 (2021) 118325, https://doi.org/10.1016/j.jlumin.2021.118325.